SAND2011-9065C

PROGRESS IN FIRST PRINCIPLES MODELING OF HPM EFFECTS

Larry D. Bacon, Jeffery T. Williams, Michael J. Walker, and Alan Mar

Sandia National Laboratories[1]

ABSTRACT

The past few decades of research into RF Directed Energy (RFDE) have witnessed the development of analytical and computational tools for modeling High-Power Microwave (HPM) effects that are capable of nearly complete electrical and mechanical characterizations of entire systems. These developments include advances in numerical electromagnetics and semiconductor physics, multiphysics modeling, meshing and gridding tools, and sheer computing power. We have progressed from analyzing nearly-canonical coupling problems to fully-coupled electromagnetic-electrothermal-device physics models of small but realistic systems. We must now ask 'How deterministic can we make our assessment of RFDE effects?' We must be able to estimate, within acceptable bounds, their variability and repeatability. Even with precise knowledge of the physical geometry of the target, there remains significant variability and strong orientation dependence of RFDE effects due to the multiple ports-of-entry feeding the terminal pairs of interest. This paper will explore our progress in predicting end-to-end effects from *first principles* – modeling as much of the physics as is required to capture the effects that are significant in a given problem. We will focus on the derivation, implementation, and validation of an Active Thevenin Equivalent Network Approach (ATHENA) to solving the linear coupling and non-linear circuit response self-consistently and efficiently.

KEYWORDS:

HPM effects prediction, multiport equivalent circuit, modeling.

NOMENCLATURE

V	vector of port voltages, [V]
Z	impedance matrix, [Ω]
I	vector of port currents, [A]

[1] Sandia is a multiprogram laboratory operated by Sandia Corporation, a Lockheed Martin Company, for the United States Department of Energy's National Nuclear Security Administration under contract DE-AC04-94AL85000.

$\mathbf{V_{oc}}$	vector of open-circuit voltages, [V]
$\mathbf{Z_{th}}$	vector of Thevenin equivalent impedances [Ω]

INTRODUCTION

Electronic systems by necessity – to be of any use – interface with the physical world. If these systems see, hear, navigate, or monitor, they must observe low-level analog signals, amplify them, and process them at moderately higher amplitude levels using either analog or digital circuitry. The systems then typically respond by controlling, maneuvering, or displaying information. These response processes are performed at even higher voltage, current, or power levels. High-Power Microwave (HPM), or Radio Frequency Directed Energy (RFDE), systems seek to interfere with these electronic systems, typically using unintended ports-of-entry for the RF energy. To be tactically useful, RFDE effects must be predictable to within an acceptable margin, even with incomplete knowledge of the target. They must be both robust and repeatable, and it is very advantageous if they are also verifiable.

At present, RFDE effects prediction is semi-empirical, comparing calculated fluences with previously-measured effects thresholds. But the very rapid rate of change of electronic systems – especially of commercial off-the-shelf (COTS) systems – make results from semi-empirical approaches highly perishable at best, and quickly irrelevant at worst. Naturally, there is a limit on how far measured effects data can be interpolated or extrapolated.

We need the ability to predict RFDE effects from first principles, which we define as modeling as much of the physics as is required to capture the effects that are significant in a given problem, validated against measurements of example systems.

First principles models give an understanding of *why* a scenario leads to the results it does. Estimates based on measurements can be interpolated as far as the *data* upon which they are based is valid. First principles models can be interpolated or extrapolated as far as the *physics* upon which they are based is valid. They also allow the details of the target that dominate the response to be identified and their impact on the variability of the response and effect margins to be addressed.

TECHNICAL APPROACH

Understanding HPM effects on electronic systems requires an understanding of the physics of four basic areas:

1. Coupling – how does the energy get into the target?
2. Energy Distribution – how much energy makes it to a critical component (usually a semiconductor device) through either direct illumination, wires, cables, or printed circuit traces?
3. Device Interaction – how does the energy affect the component (bias shift, rectification, frequency pulling)?

4. System Impact – how is the electronic system affected by this interaction?

Much of the previous HPM coupling work has assumed *weak coupling* between the electromagnetic problem and the circuit problem – that the nonlinear circuit load does not affect the linear electromagnetic coupling. At HPM power levels, though, the changing impedance of the nonlinear circuit elements presents *changing boundary conditions* for the coupling and energy distribution. The various parts of the problem influence each other. *We need an efficient but accurate method of incorporating this changing electromagnetic (EM) coupling into the nonlinear circuit solution.*

Others (e.g. Bayram and Volakis 2007) have approached this problem using a Hybrid Scattering Matrix technique. A disadvantage of this approach is that it is very difficult to implement and to relate to measurements.

The approach we have taken is an Active Thevenin Equivalent Network Approach (ATHENA) to the linear EM problem. Ports are essentially terminal pairs defined at reference planes that are physically close enough compared to the wavelength that unique voltages and currents can be defined, as indicated in Figure 1.

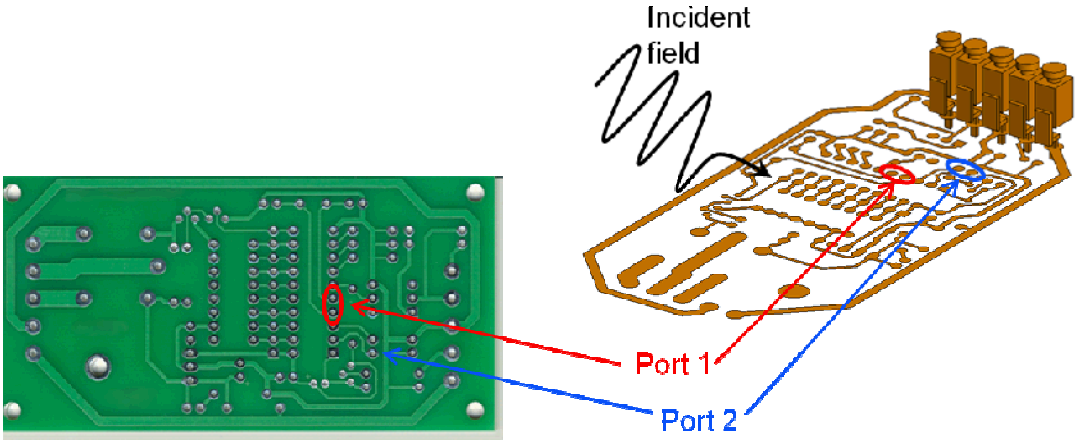

Figure 1. Ports Defined on a Simple Printed Circuit Board.

This approach is general and can be applied to N-ports. However, for demonstration purposes, the examples presented here will be for 1-port and 2-port networks. For the representation shown in Figure 2, the port voltages and currents are given by

V is the vector of port voltages, which is what we are solving for, [**Z**] is an impedance matrix, which, in the frequency domain is complex, the rows of which relate the currents **I** at all of the ports to the voltage produced at the port corresponding to that row. For a fixed geometry, it is a function only of frequency. This matrix is readily determined using standard frequency, time-domain, or even measurement techniques. $\mathbf{V}_{oc}$ is the vector of open circuit voltages induced at each port by the

incident RF. $\mathbf{V_{oc}}$ is a function of frequency, polarization, and the angles of incidence. For a two-port network,

Since the open circuit voltages are dependent upon the angles of incidence and polarization of the incident field, we need to consider all angles and polarizations to determine $\mathbf{V_{OC}}$ completely. Using the reciprocity theorem, however, the open circuit voltages at each port can be determined by *driving* the port with a fixed current and measuring each component of the radiated electric field, a much simpler procedure than simulating or measuring the response at all angles and polarizations. From reciprocity, the radiation pattern can be scaled to yield the open circuit voltage for polarization component p:

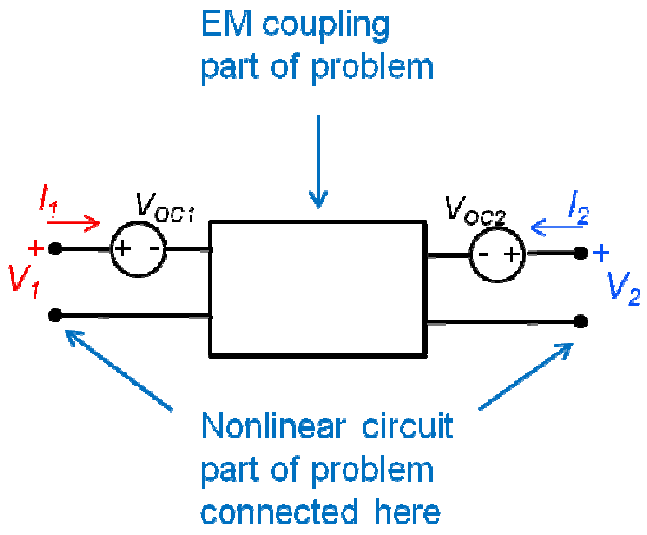

Figure 2. Active Thevenin Equivalent Network Representation of a Two-Port.

RESULTS

As an example of an ATHENA implementation, we initially considered a single-port problem for simplicity in validation against analytic solutions and experiment. The load circuit is modeled as a simple linear or nonlinear device such as a resistor or diode. As a test case, we used electric field coupling to a single wire transmission line above a ground plane, a distributed excitation example from (Paul 2008, 636). The geometry of the problem is shown in Figure 3. The 20mil diameter wire is 1m long and suspended 2cm above the ground plane. A 1kΩ load resistor is attached to the far end. The near end, which we will consider to be the single port in our problem, has a 500Ω resistive

load. Both of these loads are higher than the 303Ω impedance of the line itself, so the voltage reflection coefficient at each end is positive. The incident field is shown in Figure 4.

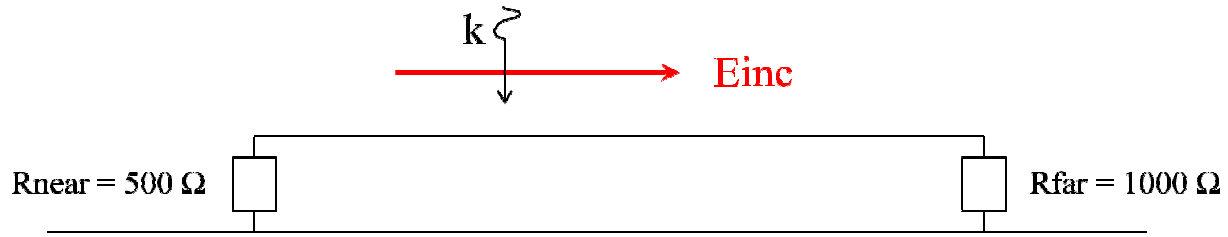

Figure 3. Single Wire Transmission Line over a Ground Plane.

The electric field is incident normal to the ground plane and aligned with the transmission line axis. It rises from zero to maximum in 1ns. For the resistive load cases considered below, the maximum amplitude is 1V/m. For the diode case, the amplitude was increased to 100V/m in order to provide enough excitation to turn on the diode.

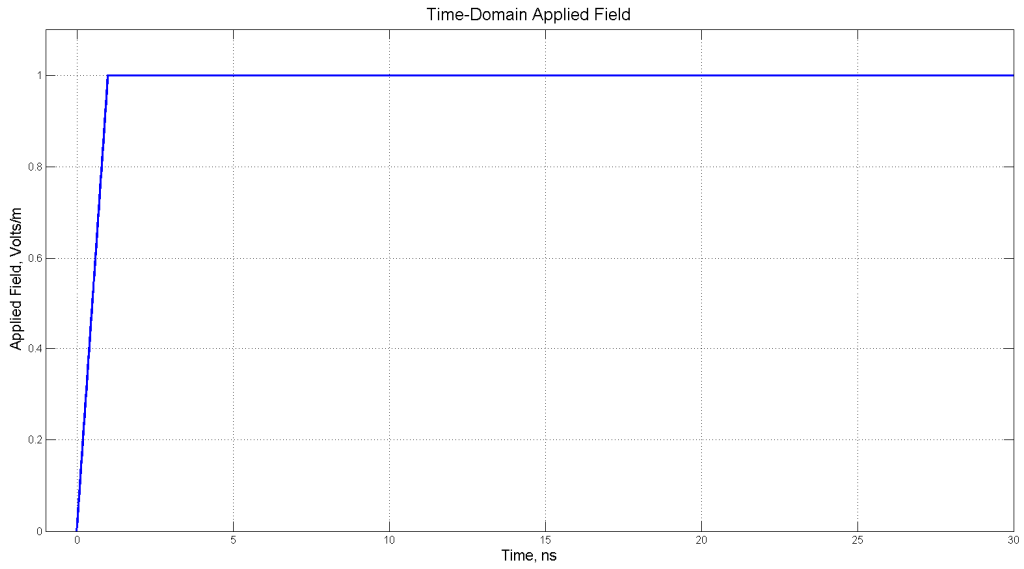

Figure 4. Incident Electric Field, 1ns Risetime, Amplitude 1 V/m or 100 V/m.

We will progress toward implementing and validating ATHENA through four example solutions of this problem: the direct solution entirely in the frequency domain, the equivalent circuit solution in the frequency domain, the equivalent circuit solved in the time domain by convolution using transformed frequency domain data, and, finally, the equivalent circuit solution in the time domain using convolution and iteration for a nonlinear load. We are working our way toward illustrating the ATHENA method with nonlinear loads, validated against known solutions.

First is the direct solution, where two different frequency domain methods, 1) a fully three-dimensional electromagnetic simulation of the problem using the method-of-moments wire code NEC, and 2) the Telegrapher's Equation with distributed excitation (ODE) solution from (Vance

1978), are solved entirely in the frequency domain. The frequency-domain solution is possible since both the electromagnetics and the circuit are linear. The frequency domain data extend from 1 MHz to 3000 MHz in 1 MHz steps. For comparison, a time-domain modal solution of the transmission line, implemented in LineCAP (Bacon and Toth 1989), was used to compute the resulting waveform directly in the time domain.

In this first solution, NEC was used with the actual terminations, R_{near} and R_{far}, to compute the broadband response for the voltage across R_{near} in the frequency domain. This response was read into a Matlab script and multiplied by the spectrum of the incident waveform to compute the spectrum of the voltage at the near end. This was then inverse transformed to generate the time-domain waveform of the voltage across R_{near}. Using the analytic frequency-domain solution of the ODE from Vance, this same process was implemented in Mathematica for the ODE. These waveforms agreed with the published results. An example of the frequency domain calculations is shown in Figure 5. It shows the NEC (blue) and the Vance ODE (red) spectra for the open circuit voltage at the near terminals. Resonances of the transmission line loop are apparent. The two solutions are nearly identical at low frequencies, but they diverge slightly as the frequency increases. This is due to the 2cm vertical lines at the terminals on each end, which are included in NEC, but neglected in the transmission line models, which assume pure TEM fields.

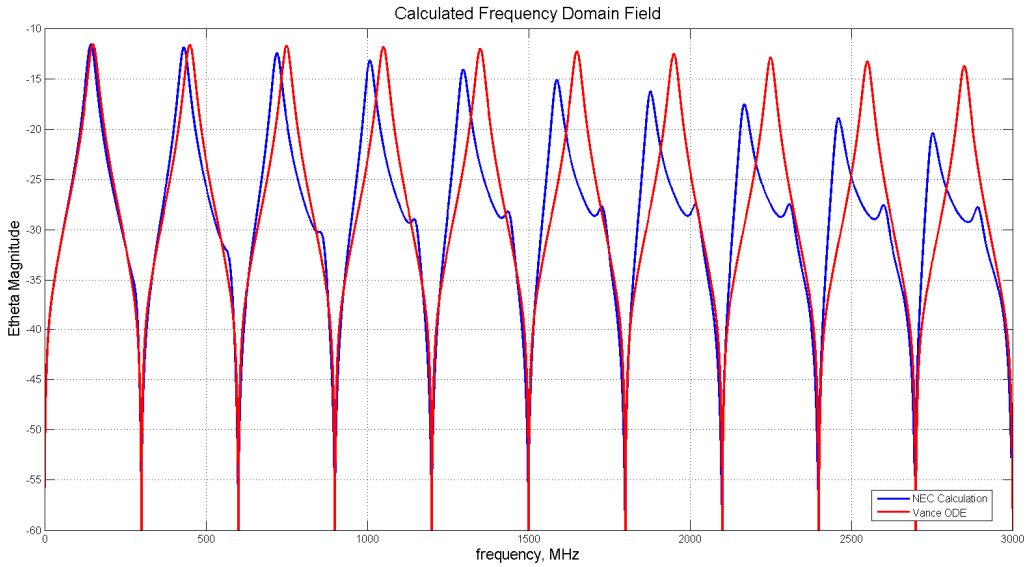

Figure 5. Frequency Domain Magnitude of Voc (dB).

In the second solution approach, we used the frequency-domain calculations of the open-circuit parameters V_{oc} and Z_{th} to solve for the voltage at the near end using a Thevenin equivalent circuit for the transmission-line/R_{far}/E_{inc} combination. We removed R_{near} and calculated V_{oc} and Z_{th} at the terminals where it had been connected, again in the frequency domain using NEC and the ODE solution. Again, since the load R_{near} is a linear resistor, the Thevenin equivalent circuit loaded by R_{near} can be solved in the frequency domain and then inverse transformed to find the time-domain solution. The time-domain solution for the three methods is shown in Figure 6. The structure of this

resulting time-domain waveform is easily understood. The incident field excites the line along its entire length simultaneously, due to its normal angle of incidence. Since the incident electric field is polarized along the wire, the voltage at the near end is negative with respect to the ground plane, since the field pulls positive charge from the ground through R_{near}. The voltage induced at the far end is positive, since charges are pushed through R_{far} toward ground. Each of these terminal voltages launches a voltage wave traveling along the line at the speed of light. These waves reach the other end of the line 3.3ns later and are reflected. Since both R_{near} and R_{far} exceed the 303Ω impedance of the line, the reflection coefficients are positive. All of this behavior, of course, is contained in the magnitude and phase of the frequency response of the electromagnetic system, combined with the *v-i* characteristics of the terminal loads. The slightly longer ring time of the NEC solution, as mentioned above, is visible. Otherwise, the solutions are in excellent agreement with each other and with the solutions in Paul (2008). This first solution gives us a baseline to compare to subsequent solution methods. This result demonstrates that our equivalent circuit is working properly.

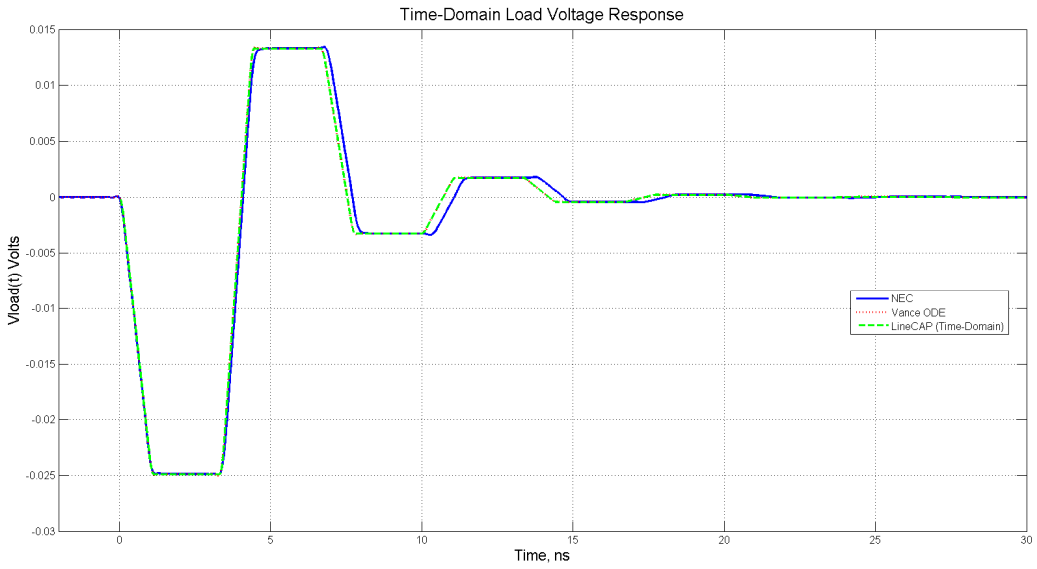

Figure 6. Waveform for Frequency Domain Solution of Linear Problem, with Time Domain Modal Solution for Comparison.

In the third solution approach (ATHENA), we transform the V_{oc} and Z_{th} results into the time domain *before* solving the linear circuit using convolution. Figure 7 shows the ODE and LineCAP results. This step allows us to validate our implementation of the convolution.

Finally, we replaced R_{near} with an ideal diode, as shown in Figure 8. The *v-i* terminal behavior was assumed to follow the ideal diode equation. The solution technique is the same as in the previous example, except at each time step in the convolution the terminal voltage and current are iterated until both the linear circuit (loaded transmission line) and the nonlinear component (diode) *v-i* characteristics are satisfied. This final result is shown in Figure 9, with the open circuit voltage also shown for comparison. When the voltage first goes negative, the diode is biased off, so the load is essentially an open circuit. Thus, V_{oc} and the diode response track each other.

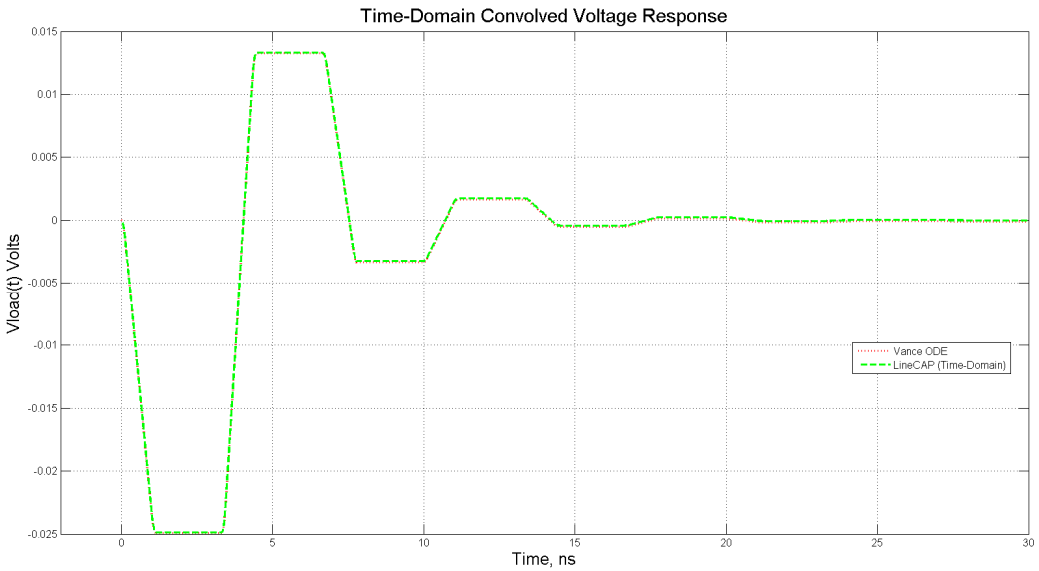

Figure 7. Time Domain Convolution Solution, Linear Load.

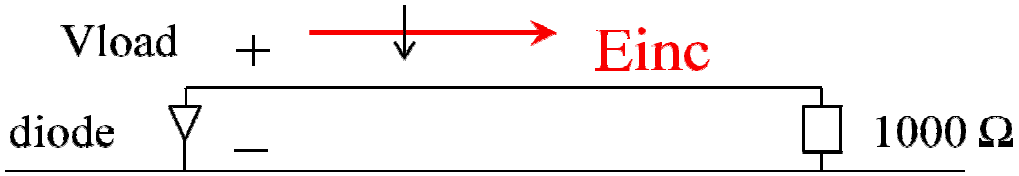

Figure 8. R_{near} replaced with Ideal Diode.

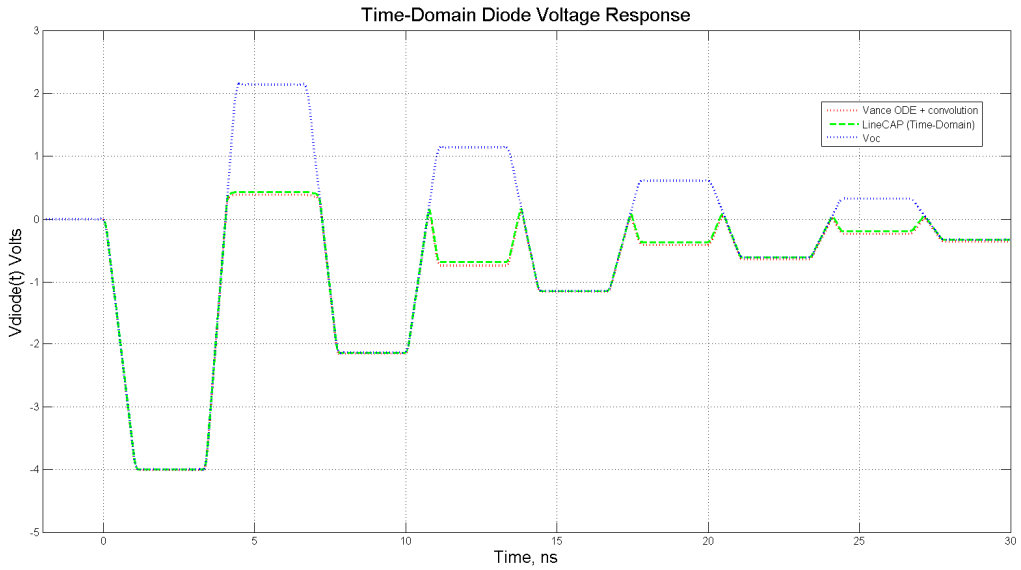

Figure 9. Response for Ideal Diode Load, with V_{oc} for Comparison.

As the voltage swings positive due to the arrival of the voltage wave excited at the far end, the diode turns on and clamps the voltage level to its saturation value. This results in a negative reflection coefficient, since the impedance of the saturated diode is much lower than the transmission line impedance. The negative wave launched at this time reappears each time V_{oc} swings positive since it is reflected back to the input from the far end. Note that the ATHENA results and the direct LineCAP results for this nonlinear case are nearly identical, with only a slight offset that depends upon the time-step chosen.

This physical insight into both the electromagnetic and circuit behavior of system is a benefit of choosing this very simple example, but the very same process could be used for any one-port device, regardless of its physical complexity. For example, frequency domain results for one of the ports in Figure 1 could be substituted without any changes to the scripts or analysis process. Ringing and cross-coupling on the printed circuit board traces would be visible – but would be more difficult to interpret while verifying the approach and coding.

To complement the modeling, we have measured a physical implementation of this line in a Gigahertz Transverse ElectroMagnetic (GTEM) cell. Measurement results are shown in Figure 10 along with a NEC calculation. Agreement is good at low frequencies, but departs significantly above approximately 1.5 GHz. We have verified that this is due to mutual coupling between the loop and its images in the floor and septum of the cell. We are working to incorporate these images in the model for higher fidelity to the measurement.

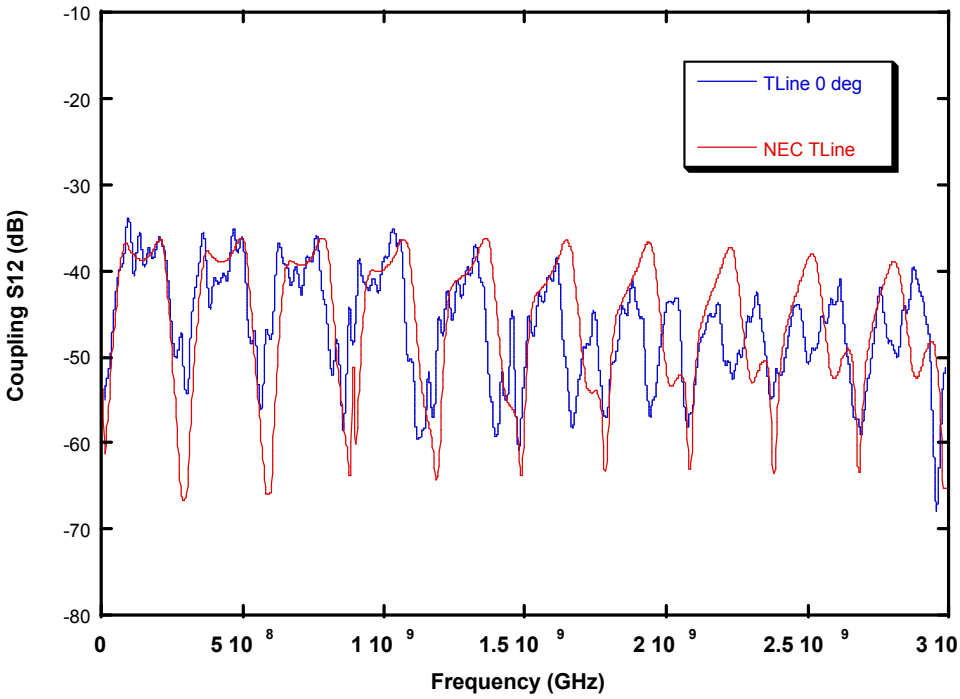

Figure 10. Frequency Domain Measurement of Transmission Line Response.

CONCLUSIONS

In this work, we have established and documented the theoretical foundation of the Active Thevenin Equivalent Network Approach. We have defined and run test and validation problems in very simple circuit codes to debug and validate the algorithm for single port devices with both linear and nonlinear loads. Further work will extend the testing and validation to N-port networks. We will continue implementing and testing the Active Thevenin Equivalent Network Approach, an efficient technique for incorporating EM fields self-consistently into circuit simulation.

Existing Spice-like circuit solvers could be applied to the linear and non-linear loads in this approach, but a new circuit device would have to be added to represent the Thevenin equivalent network of the coupled-field source. A new device representing the field coupling is being developed to run in the open-source Spice ngspice for initial testing. Implementing the algorithm in ngspice will allow later scaling to a parallel Spice solver such as Xyce (Keiter et al. 2008).

REFERENCES

Bacon, L. D., and R. P. Toth. 1989. LineCAP: Cross-coupling on pc board traces including discontinuities and circuit elements. Sandia Report SAND89-0037. Sandia National Laboratories, Albuquerque, New Mexico. Printed June, 1989.

Bayram, Y. and J. L. Volakis. 2007. Hybrid S-parameters for transmission line networks with linear/nonlinear load terminations subject to arbitrary excitations. *IEEE Trans. Microwave Theory and Techniques* Vol. 55, No. 5 (May), pp. 941-950.

Keiter, E. R. et al. 2008. Xyce parallel electronic simulator : Users' guide. Sandia Report SAND2008-6461. Sandia National Laboratories, Albuquerque, New Mexico. Printed February, 2009.

Paul, Clayton R. 2008. *Analysis of multiconductor transmission lines, 2nd ed.* Wiley-IEEE Press, John Wiley & Sons, Inc., Hoboken, New Jersey. 780 pp.

Vance, Edward F. 1978. *Coupling to shielded cables*. Wiley. New York, New York. 183 pp.